Printed in the Republic of Korea
ANALYTICAL SCIENCE & TECHNOLOGY
Vol. 36 No. 2, 70-79, 2023
https://doi.org/10.5806/AST.2023.36.2.70

Synthesis, spectral, thermal, structural study and theoretical treatment of new complexes of mannich base with Ni(II) and study of cytotoxicity effect on (Hepa-2) cell line and antimicrobial activity

Omar H. Al-Obaidi★

Department Of Chemistry, College Of Science, University of Anbar, Ramadi, Iraq

(Received August 15, 2022; Revised October 27, 2022; Accepted October 29, 2022)

Abstract: The synthesis of the Mannich base as a ligand (L) N-(morpholino (phenyl) methyl) acetamide is the subject of this study. Elemental analyses, FT-IR spectra, UV-vis, ^{1}H-NMR, and magnetic measurements were used to confirm the synthesis of the $[Ni(L)_2]Cl_2$ complex, thermal analysis (TG/DTG), atomic absorption, and scanning, and structurally explained as electron microscopy (SEM), and X-ray powder diffraction (XRD) methods. The melting point of the complex and its molar conductivity were also measured. The suggested geometries of the complexes formed have a tetrahedral structure, according to the data acquired using various techniques. Theoretical approaches to the complex formation have been investigated. For molecular mechanics and semi-empirical calculations, the HYPERCHEM6 program had been used. The effect of the novel Ni(II) complex on the cancer cell Hepa-2 (human hepatocellular ademocarcinoma), that is the human laryngeal cancer, was studied. It has been found that these ligand and complex have potent effects on the cancer cell. The antibacterial activity of the free ligand and its complex was evaluated against two kinds of human pathogenic bacteria. The first category is Gram-positive (Staphylococcus aureas, epiderimids), whereas the second group is Gram-negative (Psedamonas aeruginosa, Escherichia coli) (from the diffusion method). Finally, it was discovered that various chemicals had varied growth-inhibiting effects on bacteria.

Key words: Mannich base, biological activity, complex, spectroscopic studies, X-ray structure, thermal analysis

1. Introduction

The chemistry of the Mannich base and its derivatives has attracted the attentions of coordination chemists[1] due to their potential as ligands for a wide range of metal ions. Studies on Mannich base-ligand complexes are of importance, with particular interest in complexes between transition metal ions.[2] Recently, metal ions have a crucial part in most biological processes, according to research in bioinorganic chemistry. Mannich bases with six-membered ring structures, are still used in the manufacture of vitamins and medications.[3] In some cases, metal complexes of clinically important ligands can be more impactful than free ligands.[4] It is widely accepted that heterocyclic compounds play an important role in a variety of

★ Corresponding author
Phone : +974-07803678193 Fax : +974-07803678100
E-mail : edw.laith21973@uoanbar.edu.iq; dromaralobaidi@yahoo.com

biological systems. As a result, it is not unexpected that numerous authors have investigated heterocyclic compounds as ligands in coordination compounds containing several central atoms.[5-7] To provide novelty to medical research, the complexes and their structures have been characterized and tested to determine whether to have anti-disease effects. Many Mannich base derivatives have been shown to have biological action,[8] bactericidal[9] and anticancer activity[10] and several others have been reported to have anti-inflammatory,[11] antispasmodic,[12] antiviral,[13] antifungal,[14] antitumor[15] and anti-HIV properties.[16] As part of this study, Ni II with N-((2-hydroxyphenyl (morpholino) acetamide) complex was synthesized and the structural features were described using X-ray diffraction investigations, FT-IR spectra, UV-VIS spectra, elemental analyses, magnetic measurements, and TGA/DTG curves. The breakdown paths of the examined compound are addressed in connection with the spectroscopic data that is available.

2. Experimental

2.1. Instrumentation and materials

2.1.1. Instrumentation

The FT-IR spectra were obtained using CsI and KBr discs on an IR Prestige 21 SHIMADZU infrared spectrophotometer, the UV/VIS spectra were acquired using a twin beam/D80 Biotoch D80/USA spectrophotometer, Atomic absorption Sauant AA GBC was used for elemental analysis. A METTLER TOLEDO conductivity meter was used to measure electrical conductivity. An electrically heated block apparatus (Gallen Kamp) was used to determine melting points. The Perkin Elmer TGA 4000 system was used to perform thermal analyses (TGA, DTG) In platinum crucibles as the sample vessel, a dynamic nitrogen atmosphere (100 mL/min) at a heating rate of 10 °C/min was applied, with-Al_2O_3 as a reference.

Magnetic susceptibility measurements were carried out at room temperature using a Johnson Matthey magnetic balance, model Gouy, and a quantum-designed physical property measurement system (PPMS). Images of scanning electron microscopy (SEM) and X-ray detection (DX) from MEIJI, Japan, were captured using Joel SHIMADZU RD-6000 equipment with a 20 KV accelerating voltage. X-ray powder diffraction analysis, target copper with secondary monochromate, was used to record X-ray diffraction patterns for the complex in Jordan's capital, Amman.

2.1.2. Materials

All chemicals used were analytical reagent products. BDH Chemicals provided $NiCl_2.6H_2O$, Morpholine, Acetamide, and Benzaldehyde, while sigma Aldrich provided absolute ethanol, diethyl ether, and DMSO.

2.2. Preparation of the ligand N-(morpholino (phenyl) methyl) acetamide (L)

The ligand (L) was prepared according to the literature.[17] Morpholine (8.7 g, 0.1 mol), alcohol (50 mL), acetamide (5.9 g, 0.1 mol), benzaldehyde (10.60 g, 0.1 mol) were slowly mixed under vigorous stirring (1 hr) in ice bath until it turned yellow. Filtered solid was washed with water, dried, and recrystallized from alcohol. 87 % yield, yellow powder, M.P. 136-138 °C, IR (KBr disk) shows absorption at 1650 cm^{-1}

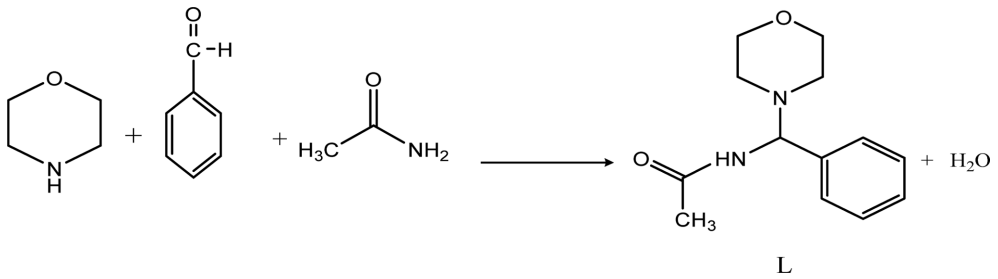

L

Fig. 1. Synthesis of ligand.

(C=O), 1118 cm^{-1} (C-N-C), 3256 cm^{-1} (N-H). UV-Vis shows max in (DMSO) at 218 nm and 275 nm. C.H.N. analysis; C=66.62 (Cal. 66.64), H=7.70 (Cal. 7.74), O=13.61 (Cal. 13.66) and N=11.91(Cal. 11.96) (*Fig.* 1).

2.3. Preparation of complexes

Corrected as to "5 ml (2 mmol) hot ligand solution in absolute ethanol was added to 5 ml (1 mmol) hot metal chloride solution, then, for 2 hours, the mixture was stirred and refluxed. The color of the solution immediately changed. After cooling the reaction mixture, the solution was either vacuum evaporated or stored at room temperature overnight. From absolute ethanol, the precipitate was vacuum-collected, washed, and recrystallized. Yield 80 %, light brown powder, M.P. 98.0-100. 0 °C, IR (CsI disc) demonstrates absorption at 1630 cm^{-1} (C=O), 1111 cm^{-1} (C-N-C), 3255 cm^{-1} (N-H), C.H.N. analysis; C=56.52 (cal. 56.59), H=6.65 (cal. 6.79), N=9.37 (cal. 9.43), Cl= 11.90 (cal. 11.93), O= 5.35 (cal. 5.38) and Ni=9.80 (cal. 9.88).

2.4. Investigation of the biological activity of the ligand and its metal complex

2.4.1. Investigation of the cytotoxic effect on cancer cell lines

In the laboratory, a type of cancer cell line was used to study the effect of manufactured compounds on cell growth, and thus the specifications of metal complex as antitumors are known, This research was carried out at the University of Nahrain's Biotechnology Research Center's Department of Cancer Research. All solutions are prepared in the same facility.

The MTT (dimethyl-2-thiazolyl-2,5-diphenyl-2H-tetrazolium bromide) based cell viability assay was used in to 96-well plates to assess the cytotoxic impact of ligand and complex.[18] The effect of these compounds on normal cells, namely Periodontal Ligament cells (PDL), was also investigated. The cells were cultivated in each well of a 96-well plate in a volume of 100 µL and incubated at 37 ºC. The cells were treated with the test chemicals (100 µL) at a concentration of 1mg/mL in DMSO after 3 hours and incubated for another 24 hours. Following the pipetting of the media, 10 µL MTT and 90 µL media were added to each well. After incubating the plate for 4 hours at 37 ºC, 100 µL of DMSO was added. The plate was then incubated for 30 minutes at 37 ºC before measuring absorbance at 570 nm and background at 620 nm with a microplate reader. The experiment was done three times, and the results were calculated as IC50 values using the mean of three independent values.

The rate of cell growth inhibition (the percentage of cytotoxicity) was calculated using the following equation : (inhibition rate = A-B/A*100), where A is the control optical density and B is the sample optical density.

2.4.2. Antibacterial activity

The bacteria Escherichia coli and aurous Staphylococcus-Bacteria were obtained (isolated and diagnosed in the culture laboratory at the Children's Hospital in Ramadi) and measured using the Agar-well diffusion method, followed by the Kirby-Baauer method.[19] In addition, Mueller Hinton Ager was used to test the susceptibility of bacteria to compounds, and it was prepared according to the manufacturer's instructions. After that, the dishes were placed in a 37 ºC incubator for 24 hours, and the diameter of inhibition was measured (zone of inhibition).

3. Results and Discussion

Several spectroscopic techniques were used to confirm the structures of the Mannich base ligand and its complex.

3.1. FT-IR spectra

The infrared spectra of the complexes were recorded. Absorption bands in the region of 3256 cm^{-1} correspond to stretching frequencies of (N-H). This band remained almost in the same region of the free ligand, indicating that the ligand does not coordinate through these groups.[20] The IR spectra demonstrate that the band at 1118 cm^{-1} in the spectrum of the free ligand is moved to lower frequencies in the complexes

owing to (CNC) stretching. The typical negative shift in (C-N-C) also demonstrated coordination to metal ions via the ligand's nitrogen atom (-CNC-), and complexation indicates involvement with metal ions. The ligand complex gives rise to a strong band responsible for the C=O stretch. The conjugation of the carbonyl group and the amide nitrogen results in minor frequency shifts. This mode is responsible for the strong bands observed at approximately 1650 cm^{-1}. The band in the spectrum at 1650 cm^{-1} is caused by (C=O) stretching vibrations in the free ligand. The carbonyl peak in the complex appears in the 20 cm^{-1} region. The major variation in the ligand spectrum is that the carbonyl group's C=O stretch at 1650 cm^{-1} is displaced to lower frequencies in the nickel complex. This indicates that the coordination occurs through the carbonyl group.[24] The observations indicate that the ligand is coordinated by an oxygen atom. Because of the transfer of charge from the ligand to the metal, the carbonyl stretching frequency falls to 1630 cm^{-1} when compared to the free ligand.[22] MN and MO vibrations are attributed to low-intensity bands in the 600-400 cm^{-1} range.[23]

3.2.2. 1H NMR spectra

The 1H NMR spectrum of the Mannich base ligand (*Fig.* 2), shows H1 chemical shift=7.2 ppm (m) suggested the attribution of the protons of the 1-benzene group, H2 chemical shift=6.90 ppm (m) suggested the attribution of the protons of the 1-benzene group, H3 chemical shift=5.8 ppm (d) suggested the attribution of the protons of the methine group, H4 chemical shift=2.00 ppm (s) suggested the attribution of the protons of the 1,4-oxazine group, H6 chemical shift=6.7 ppm (d) suggested the attribution of the protons of the methine group, H7 chemical shift=2.7 ppm (d) suggested the attribution of the protons of the 1,4-oxazine group, H5 chemical shift=8.6 ppm (d) suggested the attribution of the protons of the secondary amide group, H8 chemical shift=3.45 ppm (d) suggested the attribution of the protons of the tetrahydro-1,4-oxazine group.[24]

3.3. Electronic absorption spectra

The absorption spectra At (10^{-3} M) in DMSO, the electronic spectrum of the ligand and its complex was recorded. If the complexes have a different color than the transition metal salt and the ligand, this is an

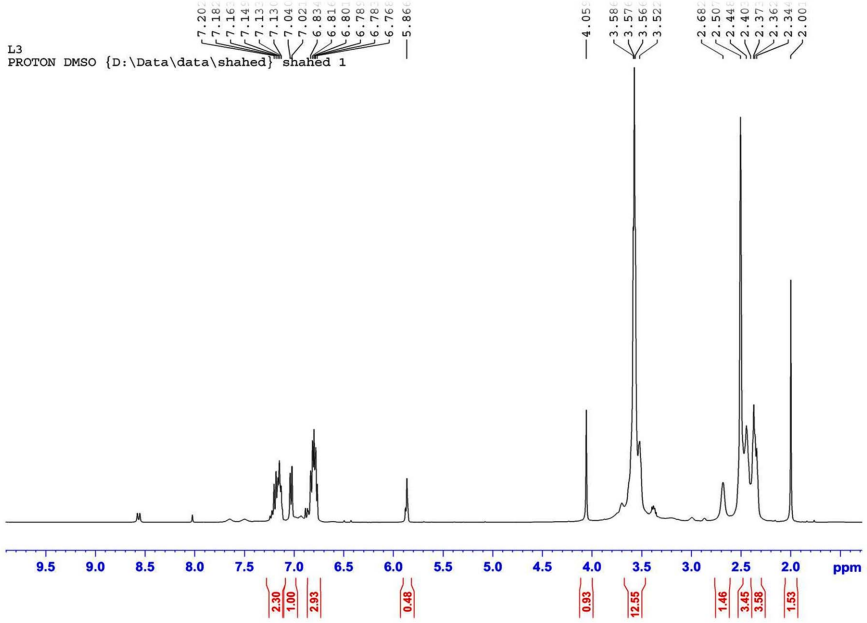

Fig. 2. 1 H-NMR spectrum of the ligand.

important indication of coordinated occurrence. Furthermore, these colored complex have different characteristic absorption bands in position, intensity, or together compared to the ligand bands, which is another indication of coordinated occurrence.[25] The UV/visible spectra of the prepared ligands (L) in ethanol at (10^{-3} M) revealed two absorption bands. The first band (218) nm representing (π-π*) is called (B band) for the phenyl group and the second band (275) nm representing (n-π*) for the C=O group.[17] The electronic spectra of the Ni(II) complex showed five bands at 10367 cm^{-1} assigned to the 3T1(F)⟶ 3T2(F) transition, 16362 cm^{-1} assigned to the 3T1(F)3 → A2, 27451 cm^{-1} assigned 1 allocated for the 3T1 (F)⟶ 3T1 (P), 30653 cm^{-1} allocated for the charge transfer transition and 36465 cm^{-1} allocated for the charge transfer transition. The coordination geometry of the Ni II ion is that of a tetrahedron with the N and O atoms of the ligand.[26]

3.4. Magnetic measurements

Magnetic measurements were carried out using the Gauy method. The value of magnetic moments was reached to 3.23 BM, this value were confirmed with value calculated from experimental data for the tetrahedral Ni(II) complex.[27]

3.5. Molar Conductance Measurements

The molar electrical conductivity of complex was measured in an organic solvent (DMSO solvent) at 25 °C, and the value of molar electrical conductivity was 77.47 ms·cm^{-1}. This value reveals to the high molar electrical conductivity. These findings support the stoichiometry of these complexes, which correspond to the general formula presented.[28]

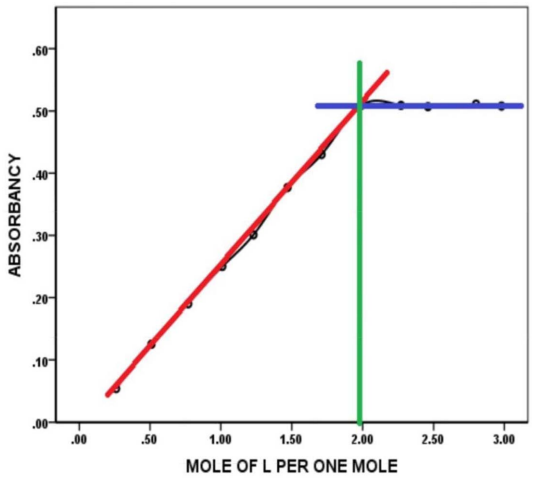

Fig. 3. Diagram of Ni(II) complex formation.

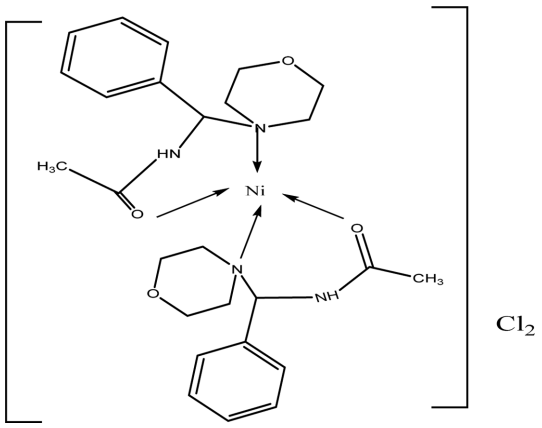

Fig. 4. The proposed structure of the complex.

3.6. The mole ratio study

One of the most popular spectrophotometry used in complicated research is the mole ratio.[29] It is a technique for determining the composition of complex in solution. The ligand (L) to metal (Ni(II)) molar ratio (2:1) is caused by absorption due to the change of the coordination ion of the ligand complex, as shown in (*Fig.* 3).

3.7. The proposed structure

The hypothesized molecular structure is based on the results of experiments for the complex formed (IR, UV/visible, molar ratio, molar conductivity, atomic absorption). As shown in (*Fig.* 4), the complex have an octahedral structure.

3.8. Complex formation and stability constant

As per the literature, the technique of molar ratio of equimolecular solutions yielded the most accurate findings for the stoichiometric composition of flavonoid complex.[29] When we plot absorbance versus ligand mole fraction, we see that a 2:1 chelate is formed. The results agreed with the data obtained using the

slop ratio approach. Absorption spectra of a 2:1 (L:M) solution were recorded to estimate the apparent stability constant of the complex, which was found to be 1.58 × 10^3 for the Ni(II) complex (*Fig.* 4).

3.9. Theoretical study

Table 1 presents the structural parameters such as; length of bonds, angle bonds, sphere, cylinder of structure and the optimized geometries. As indicated in the (*Fig.* 5), there is no apparent trend in the change of these variables' parameter. The optimized geometries for bond length and angle bond values are very close to the experimental results for the related compounds.

3.10. Thermal analysis

Analysis (*Table* 2) shows the TG-DTG curves for the Ni(II) complex. According to these curves, two moles of neutral ligand are decomposed with removal of chloride groups (exp. 10.91 %; calc. 11.00 %).

Table 1. length of bonds (Å) and bonds angles (°) for the $[Ni(L)_2]Cl_2$ molecule

Parameters			
Bond lengths (Å)		Bond angles(º)	
N(31)-C(26)	1.4380	C(35)-N(34)-C(33)	81.5826
C(26)-C(27)	1.5230	C(35)-N(34)-Ni(25)	118.0001
N(31)-Ni(25)	1.0120	C(35)-N(34)-C(1)	107.6999
N(34)-Ni(25)	1.0120	C(33)-N(34)-Ni(25)	117.9998
O(24)-H(57)	0.9720	C(33)-N(34)-C(1)	107.7000
C(17)-H(50)	1.1130	Ni(25)-N(34)-C(1)	118.0001
O(16)-Ni(25)	1.7900	C(30)-N(31)-C(26)	81.5824
C(6)-C(7)	1.3370	C(30)-N(31)-Ni(25)	118.0001
O(5)-Ni(25)	1.7900	C(30)-N(31)-C(13)	107.7000
C(4)-H(42)	1.1130	C(26)-N(31)-Ni(25)	118.0001
C(22)-O(24)	1.3550	C(26)-N(31)-C(13)	107.7001
C(37)-H(76)	1.1130	Ni(25)-N(31)-C(13)	117.9998
C(36)-H(75)	1.1130	Ni(25)-O(16)-C(15)	179.9999
C(36)-H(74)	1.1130	N(31)-Ni(25)-N(34)	109.5000
C(36)-C(37)	1.6009	N(31)-Ni(25)-O(16)	90.0001
C(35)-H(73)	1.1130	N(31)-Ni(25)-O(5)	90.0000
C(35)-H(72)	1.1130	N(34)-Ni(25)-O(16)	160.4999
C(35)-C(36)	1.5230	N(34)-Ni(25)-O(5)	90.0000

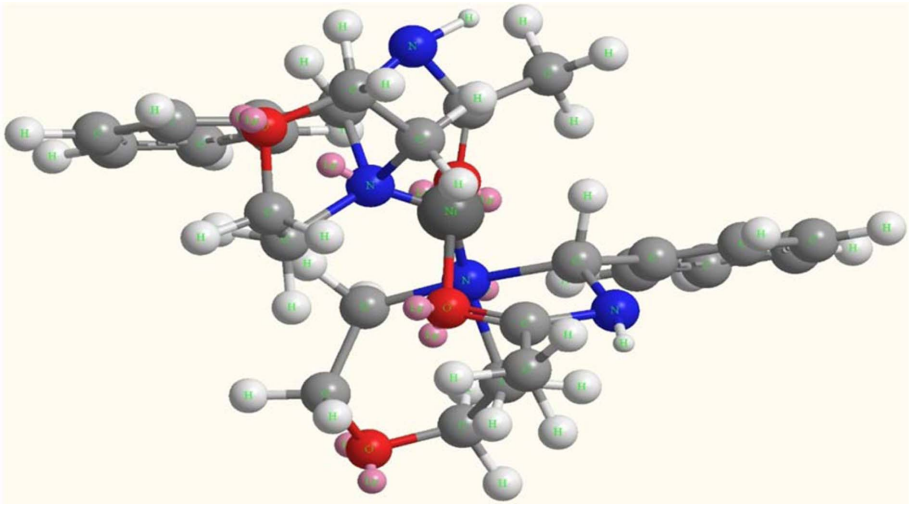

Fig. 5. Show the optimization geometry of structural for $[Ni(L)_2]Cl_2$ molecule with atoms numbering scheme.

Table 2. The TG-DTG curves of the Ni(II) complex

Complex Lost $C_{28}H_{40}Cl_2N_4NiO_2$	Decomposition	Tmax/C°	Decomposition peak DTG,C°	% Weight loss
$-Cl_2$	First stage	(65-200)	150	(11.00) 10.91
$-C_{18}H_{20}N_4O_2$	Second stage	(270-360)	260	(55.60) 55.34
$-C_{10}H_{20}$	Third stage	(535-650)	600	(21.69) 21.77
NiO	Residue			(11.57) 11.47

Then two moles of amide groups of the ligand are released from the structure with endothermic effect (exp. 55.34 %; calc. 55.60 %). Thereafter, two moles of phenyl groups are decomposed and at 535 C DTG peak is removed as an endothermic (exp. 21.77 %; calculated 21.69 %) peak. After decomposition of neutral ligands at 650 °C. Finally, nickel oxide (NiO) remains in the crucible (exp.11.47 %; calc. 11.57 %).

Table 3. Crystal data of the prepared complex

PXRD information	$NiCl_2.6H_2O$
Molecular Formula	40.13
Molecular Weight	237.69
Crystal system	Monoclinic
Space group	C2/ (12) m
Unit cell parameters (A°)	a=10.23, b=7.05, C=6.57, β=122.17
Cell volume (A^{o3})	401.09
Z(no. of molecules or atoms/cell unit)	2
θ Range (deg.)	16.12-100.8
Index ranges (hkl)	$0 \le k \le 5$-$8 \le h \le 6$ $0 \le l \le 5$

3.11. X-ray powder diffraction (PXRD) studies

PXRD patterns for the Ni(II) complex at different temperatures with formulas; $[Ni(L)_2]Cl_2$, were plotted using wavelength (Co-K 1.788970 Å) to obtain information on crystal symmetry, space group, unit cell, axis, unit cell volume, and so on. The results were analyzed using the Match program[30] and are shown in (*Fig.* 6) and (*Table* 3). From these results we can demonstrate that coordination between the ligand and Ni(II) ion took place and a new coordination compound was formed.

3.12. SEM and EDX studies

Scanning electron microscopy (SEM) is the most basic instrument for gaining an understanding of the microscopic elements of Mannich base's physical nature as a chelating agent, as seen in *Fig.* 4. While not a certified approach for validating complex formation, this tool can be used to indicate the existence of a single component in synthetic complexes. The Ni(II) complex pictures exhibit tiny particle sizes with nano-feature products. The EDX data were presents the homogenous distribution of metal ions inside the chelating agent. SEM studies have confirmed the morphology of these complexes' surfaces, revealing

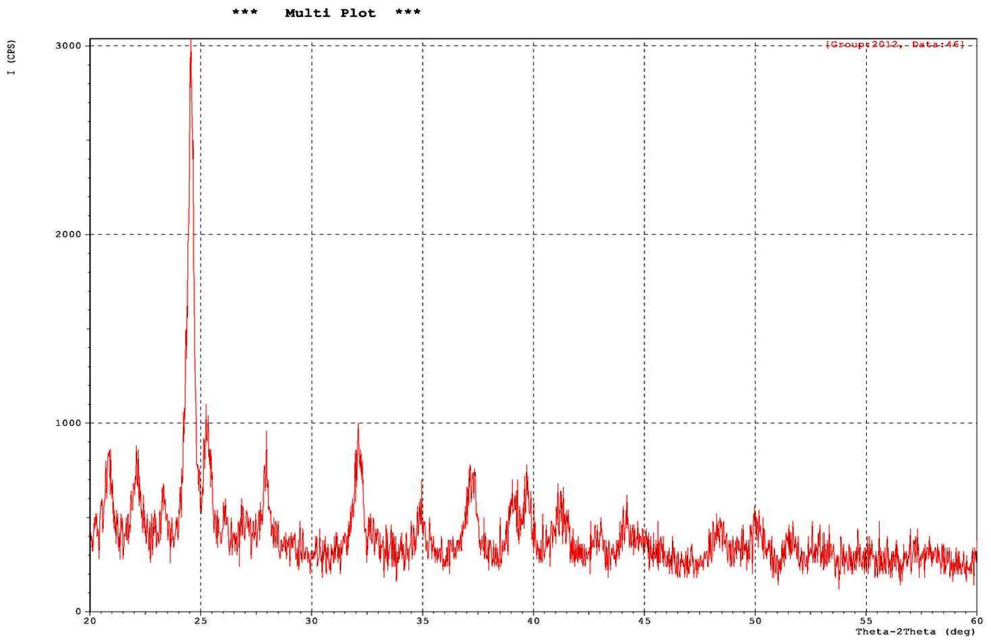

Fig. 6. Pattern PXRD for $[Ni(L_2)_2]Cl_2$.

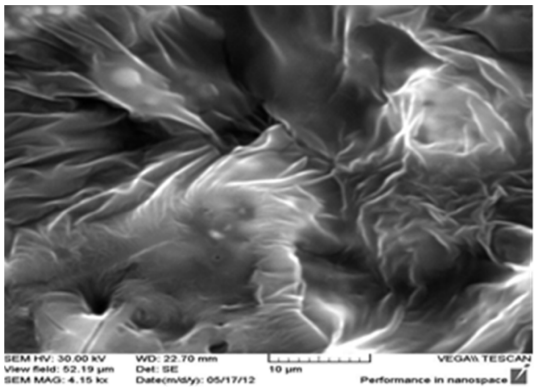

Fig. 7. SEM image of $[Ni(L)_2]Cl_2$ complex.

small particles that tend to form agglomerates with different shapes than the starting materials. The peaks of these complexes' EDX profiles, shown in (*Fig.* 7), correspond to all constituents of the complex's molecules, which were clearly identified, confirming the postulated structures.

3.13. Cancer cytotoxic effect studies

Cancer cell types were utilized in the laboratory to analyze the effect of complex on cell proliferation in order to determine the properties of complex as anti-tumor agents. Cancer cell line type (Human Hepato-cellular Ademocarcinoma) (Hepa-2) used. We determine the fraction of cell counts within ideal growth circumstances without introducing any substances in this procedure, hence the outcome is the control group (control). Then compound are added to know their effects on cell growth in selected lines. The result is analyzed statistically by one-way ANOVA. The following results, as shown in (*Fig.* 8), showing the influence of compounds on the cell number ratio using a cell line (human hepatocellular ademoca-rcinoma) (Hepa-2), results clearly reveal that the prepared complex has the largest influence on the proportion of Growth cell number, and the effect was significant (P 0.05).

The results in (*Fig.* 8) show that novel complex have a cytotoxic effect on cancer cell lines by increasing the inhibitory rates with increasing concentration, similar to the effect of anti-cancer cis-platinum. In this study, we propose that the new Mannich base ligand complex have an inhibitory effect, similar to that of Tsuda *et al.*[31] which was studied in colon and liver cancer in mice and resulted in DNA damage after a brief administration of a relatively high dose. Carcinogenicity was discovered after a long period of treatment with low doses. Kenyon *et al.*[32] showed copper concentrations reported in tumor tissues, the organic ligand (bis-8-hydroxyquinoline) formed strong inhibitors inducers when linked to cellular tumor copper. The novel complex exhibited a comparable impact to cis-pt, which might be attributed to cis-pt binding to and cross-linking of DNA, resulting in opoptosis (programmed cell death).[33]

3.14. Antimicrobial activities

The activity of the complex was investigated at various concentrations and with two distinct kinds of harmful bacteria (Staphylococcus epiderimids, Staphylococcus aureas) and (Psedamonas aeruginosa, Escherichia Coli). A zone of inhibition greater than 6 mm showed antimicrobial activity. For Staphylococcus aurous and Escherichia coli, the complex revealed a superior efficiency (*Fig.* 9). When the value of Ligand was compared to that of the complex, it was observed that the metal complex had more antimicrobial property

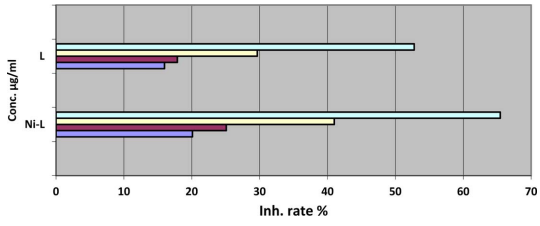

Fig. 8. The comparison of inhibitory rate treatments (Human Hepatocellular Ademocarcinoma) (Hepa-2).

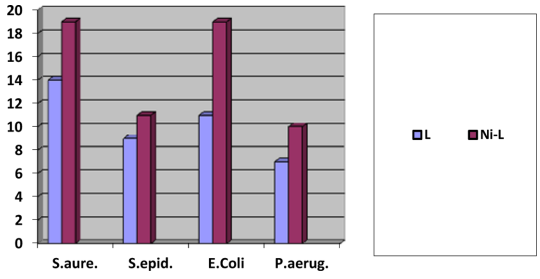

Fig. 9. The effect of the complex on the growth of bacteria.

than Ligand. The overtone notion can be used to explain the enhanced activity of the complex[34] and the Tweedy chelate theory.[35] Furthermore, as shown in (*Fig.* 9), Nickel complexes were more active against the bacteria tested than ligand.

4. Conclusions

The presence of nitrogen and oxygen atoms in the structure of an organic chelating agent has led to some fascinating discoveries in the study of coordination compounds. Prepared Mannich base ligand and its Ni(II) complex. Several spectroscopic methods were used to explore the synthetic and structural properties of the aforementioned novel kind of tetrahedral complex. Solution spectrophotometric studies show that only a mononuclear complex with a 2:1 ligand to metal stoichiometry can be obtained with a moderate stability constant. The biological activities of ligand and their metal complex against four different bacteria species were investigated,

This comprised gram positive (+Ve) bacteria (Staphylococcus epiderimids, Staphylococcus aureas) and gram negative bacteria (-Ve) (psedamonas aeruginosa, Escherichia coli) are grown and used as a control for the disk sensitivity test, demonstrating that the inhibition has a distinct effect on the development of the bacteria. The effect of the new Ni(II) complex with the Mannich base ligand on the cancer cell Hepa-2 was studied, it was revealed that this ligand and complex have powerful anti-cancer properties.

Acknowledgements

The author are grateful the Anbar University (www.uoanbar.edu.iq) and its great academic staff for providing the essential technical and academic help for this study. The author would like to thank the Department of chemistry college of science at the University of Jordan for their support.

References

1. M. N. Hughes, 'The Inorganic Chemistry of Biological Processes', 2nd Ed., John Wiley and Sons, New York, 1988.
2. M. Tramontini and L. Angliolini, 'Mannich Base: Chemistry and Uses', 17-20, CRC Press, Boca Raton, 1994.
3. P. J. Sadler and Z. Gua, 'Metals in Medicine', 1st Ed., Angew Chem. Int., 1999.
4. Robert Crichton, 'Biological Inorganic Chemistry', 3rd Ed., Elsevier B.V. Academic Press, 2019.
5. Michael Moustakas, *Materials*, **14**(3), 549 (2021).
6. A. J. Abdulghani and N. M. Abbas, *Bioinorganic Chemistry and Applications*, **2011**, Article ID 706262 (2011).
7. M. Sugumaran and S. Sivadevi, *Journal of Pharmacy Research*, **4**(8), 2679-2681 (2011).
8. M. J. Pelezar E. S. Chan, and N. R. Krieg, 'Microbiology', 5th Ed., McGraw Hill, New York, 2001
9. B. S. Holla, M. K. Shivananda, M. S. Shenoy, and G. Antony, *Il Farmaco*. **53**, 531- 535 (1998).
10. B. S. Holla, B. Veerendra, M. K. Shivananda, and B. Poojary, *Eur. J. Med. Chem.*, **38**, 759-767 (2003).
11. O. Bekircan and H. Bektas, *Molecules*, **13**(9), 2126-2135 (2008).
12. J. Chen, X. Y. Sun, K. Y. Chai, J.
13. S. Lee, M. S. Song, and Z. S. Quan, *Bioorg. Med. Chem.*, **15**, 6775-6781 (2007).
14. D. Sriram, T. R. Bal, and P. Yogeesswari, *Med. Chem. Res.*, **14**, 11-28 (2005).
15. S. N. Pandeya, D. Sriram, E. DeClercq, and G. Nath, *Eur. J. Pharm. Sci.*, **9**, 25-31 (1999).
16. O. Bekircan and N. Gumrukcuoglu, *Indian J. Chem.*, **44B**, 2107-2113 (2005).
17. T. Akhtar, S. Hameed, N. A. Al-Masoudi, and K. M. Khan, *Heteroatom. Chem.*, **18**, 316-322 (2007).
18. D. Sathya, J. S. Kumaran, S. Priya, N. Jayachandraman, S. Mahalakshmi, and A. R. Emelda, *Int. J. Chemtech. Res.*, **3**, 248-252 (2011).
19. R. I. Freshney, 'Culture of Animal Cells', 3rd Ed. Wiley, New York, 2000.
20. J. Vandepitte, K. Enghack, P. Poit, and C. Heuk, 'Basic Laboratory Procedures in Clinical Bacteriology', WHO, Geneva, 1991.
21. K. Nakamoto, 'Infrared and Raman Spectra of Inorganic and Coordination Compounds', 6th Ed. Wiley, New

York, 2008.
22. A. K. S. Gupta and V. D. Barhat, *RJPBCS*, **3**(3), 1013 (2012).
23. C. S. Dilip, V. Thangaraj, and A. P. Raj, *Arab. J. Chem.*, **9**, S731-S742 (2016).
24. D. A. Kose, H. Necefoglu, and H. Icbudak, *J. Coord. Chem.*, **61**(21), 3508-3515 (2008).
25. K. Singh, M. S. Barwa, and P. Tyagi, *Eur. J. Med. Chem.*, **41**, 147-153 (2006).
26. D. Sutton, 'Electronic Spectra of Transition Metal Complexes', McGraw-Hill, London, 1968.
27. A. A. Alhadi, S. A. Shaker, W. A. Yehye, H. M. Ali, and M. A. Abdulla, *Bull. Chem. Soc. Ethiop.*, **26**(1), 95-101 (2012).
28. G. Efthymiou, Constantinos, I. Mylonas-Margaritis, C. P. Raptopoulou, V. Psycharis, A. Escuer, C. Papatriantafyllopoulou, and S. P. Perlepes, *Magnetochemistry*, **2**, 30 (2016).
29. R. Majid, Y. Alias, M. M. Abdi, K. Saeedfar, and N. Saadati, *Molecules*, **18**, 12041-12050 (2013).
30. L. L. A. Ntoi1 and K. G. von Eschwege, *AJCE*, **7**(2), 59-92 (2017).
31. Crystal Impact, 'Phase Identification from Powder Diffraction', Ver.1 .6c Licensed to Ankara Uni. Depart. of Geological Engineering site license(c). Match (2003-2007).
32. S. Tsuda, N. Matsusaka, H. Madaram, S. Ueno, N. Susa, K. Ishida, N. Kawamura, K. Sekihashi, and Y. Sasak, *Mutat. Res.*, **465**(1-2), 11-26 (2000).
33. G. Kenyon, G. Puja, R. Harbach, G. Wayne, and Q. P. Dou, *Bioc. Pharm.*, **67**, 1139-1151 (2004).
34. B. Stordal and M. Davey, *IUBMB Life*, **59**, 696-699 (2007).
35. I. P. Ejidike and P. A. Ajibade, *Molecules*, **20**, 9788-9802 (2015).
36. V. K. Srivastava, *Future J. Pharm. Sci.*, **7**, Article Number 51 (2021).

Author's Position

Omar H. Al-Obaidi : Professor